J. Environ. Nanotechnol.
Volume 7, No.2(2018) pp. 49 - 53
ISSN (Print): 2279-0748
ISSN (Online): 2319-5541
doi:10.13074/jent.2018.06.182313

Preparation and Characterization of Nanocrystalline Strontium - Doped $SmAlO_3$ Fast Oxide Conductors

N. Kalaivani[1], M. Rajasekhar[2*]

[1,* 2]Department of chemistry, Government Arts College, Dharmapuri, TN, India.

Received: 08.10.2018 *Accepted: 02.12.2018*

Abstract

$Sm_{1-x}Sr_xAlO_3$ ($0 \leq x \leq 0.5$) powders synthesize with use of Samarium nitrate, Strontium nitrate, Aluminum nitrate and aspartic acid (fuel) by assisted combustion method and it heat at 550˚C for 6 hours. The thermal decomposition, phase identification, surface morphology and ionic conductivity of the samples study with Thermal gravimetric Analysis./ Differential Thermal Analysis., X-ray diffraction, Scanning Electron Microscopy and four probe D.C. method respectively. The formation of $Sm_{1-x}Sr_xAlO_3$ confirm with use of Fourier Transformer Infra-red studies. The weight gain and loss performance confirm with use of thermo chemical techniques. The nanoparticle size measure with High Resolution Transmission Electron Microscope studies. The synthesize materials show the reasonable ionic conductivity. These results indicate the assisted combustion method is a promising method to prepare nanocrystalline $Sm_{1-x}Sr_xAlO_3$ for solid oxide fuel cell.

Keywords: *High Resolution Transmission Electron Microscope, Ionic conductivity, Scanning Electron Microscopy, Thermal Analysis.*

1. INTRODUCTION

The electrolyte with high oxygen ion conductivity is a key component and wide range of potential applications with including as the electrolyte as oxygen sensors in solid oxide fuel cells and acting as an oxygen-permeable membrane in catalytic systems. (Stuart A. Hayward and Simon A. T. Redfern, 2004; Fang et al. 2004). Although the research into fast oxide conductors can be traced back to the study of fluorine ion conduction in lead fluoride by Faraday (1839), commercial application high temperature solid oxide fuel cells which offers a clean, more efficient energy conventional power plant, pollution-free technology to electrochemically generate electricity at high efficiencies, the bottoming cycle of an electronic power plant, domestic water heater and power units, high power density along with a small physical size, high volumetric power density and electric vehicle can be achieved by improving the material properties used for the components (Singhal, 2000; John B. Goodenongh*, Yun-Hui Huang, 2007; Young-Hag Koh et al. 2006).

Solid Oxide Fuel Cell are highly promising energy conversion devices to improve energy efficiency to provide society with clean energy producing technology, low pollution output and great fuel flexibility. The high temperature of operation (800-1000˚C) enable the solid oxide fuel cell to operate with existing fossil fuels to give very high efficiency conversion of fuels to electricity and efficiently coupled with gas turbines. SOFCs quiet and non polluting and their inherent high efficiency leads lower green house gas emissions. (Shoucheng He et al. 2014; Singhal and Yokokawa, 2001; Minh and Takahashi, 1995; Steele and Heinzel, 2001; Singh et al. 2001).

In the present work, synthesis of $Nd_2Mo_{2-x}Ga_xO_9$nano powders which using different molar ratio by assisted combustion method. The synthesized product on phase evaluation, size and shape of the $Nd_2Mo_{2-x}Ga_xO_9$ were studied. Oxide materials with high mobility of oxygen ion receive extensive attention owing to the potential applications in solid oxide fuel cells, oxygen sensors, oxygen pumps, and oxygen-permeable membrane catalysts.

2. EXPERIMENTAL AND CHARACTERIZATION PROCESSES

The nanocrystalline$Sm_{1-x}Sr_xAlO_3$powder was synthesized by assisted combustion method with high

* M. Rajasekhar
email:

purity $Sm(NO_3)_3$ (Sigma Aldrich, >99.9%), $Sr(NO_3)_2$ (Sigma Aldrich, >99.9%), $Al(NO_3)_3$ (Sigma Aldrich, >99.9%) and aspartic acid (Sigma Aldrich, >99.9%) as fuel. All of the reagents, in requisite stoichiometric amounts of the starting materials were dissolved in the double distilled deionized water in order to obtain a homogeneous solution. This solution was kept at constant heating at 80˚C toobtain the foamy powders of $Sm_{1-x}Sr_xAlO_3$and the foamy powder was carried out in a muffle furnace at 550˚C for six hours.

3. STRUCTURAL CHARACTERIZATION ANALYSIS:

X-ray powder diffraction (XRD) data were collected at room temperature with a diffractometer (Model: Philips X' Pert MPH^R) with Cu Kα radiation. The data were recorded in the 2θ range of 10-70˚ with a 0.02˚ steps. The particle size and morphology of the produced powder was analysed with a JEOL scanning electron microscopy SEM (Model: JSM-840A) equipment with INCA was used to determine the morphology of samples.

The thermal decomposition of the polymeric precursors was characterized by perkin-Elmer TG/DTA thermal analysis (Model; Pyris Diamond). The TGA is a process which relies on measuring the change in physical and chemical properties of a sample as a function of temperature (with constant heating rate) or as a function of time (with constant temperature). It is predominantly used for determining the features of a material that exhibit either mass loss or gain due to decomposition, oxidation or loss of volatiles. Differential thermal analysis is a technique inwhich the temperature of a sample is compared with that of an inert reference material during the programmed change of temperature.

The particle size of the synthesized powder was observed by means of a JOEL transmission electron microscopy (Model: 1200 EX). The synthesized powder was analysed with FTIR spectrometry. (Agilent Cary 630 FTIR spectrometer) inwhich region of about 4000-400 cm^{-1}. The ionic conductivity of the sintered pellets were measured by a dc-four probe method in which temperatures range 200-700 ^{0}C in air.

4. RESULT & DISCUSSION

4.1 Analysis of Crystal Structure

The x-ray diffraction pattern of $Sm_{1-x}Sr_xAlO_3(0\leq x\leq 0.5)$ samples are shown in Fig. 4. 1. All the samples indicated single phase materials and the pattern indexed on the basis of the orthorhombic perovskite structure (space group: Pbnm). The sample calcined at 550°C for 6 h exhibits a single phase without any impurities. The data concluded that the lattice volume increased with increasing Sr content x. These results strongly suggested that assisted combustion method required much lower calcination energy with shorter time duration than solid state reaction method.

The average crystallite size of the sample was calculated by using Scherrer equation.

$$D=0.9\lambda/\beta \cos\theta$$

Where D is the crystallite size in nm, λ is the radiation wave length (for Cu Kα radiation=1.54 A˚), β is the broadening of the line (half width) in radians and θ is the diffracting peak angle. The average crystallite size of $Sm_{1-x}Sr_xAlO_3$nano powder is at various compositions. The particle size measured from XRD data. The smaller average crystallite size (nano particle) has been achieved by using assisted combustion method compared to the conventional solid state reaction method and other methods.

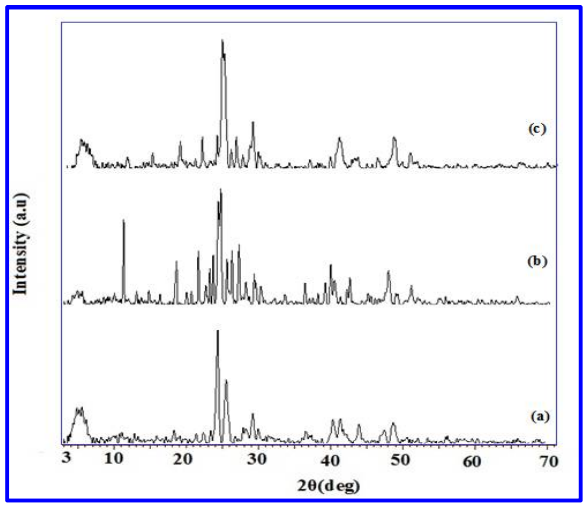

Fig 4.1: X-ray diffraction pattern of $Sm_{1-x}Sr_xAlO_3$

4.2 Scanning Electron Microscopy

Fig. 4.2. Shows SEM analysis of $Sm_{1-x}Sr_xAlO_3$ nano powder. The materials prepared by assisted combustion method using aspartic acid showed a spongy aspect and the particles linked together in agglomerates of different sizes and shapes. The loose and porous structure of these materials can be attributed to a significant gas evolution during the combustion reaction (Bansal and Zhong, 2006; Berger et al. 2007). Substantial particle growth was observed upon sintering for 6 h at 823 K. But the structure remained

highly porous which resembled the typical cathode structure for SOFC. However Gallium doping significantly improves the grain growth. The average grain size of the doped samples is 2 µm. The average crystallite size was 24 nm. The particles are not uniformly distributed. The particles of the synthesized products are in nanorange.

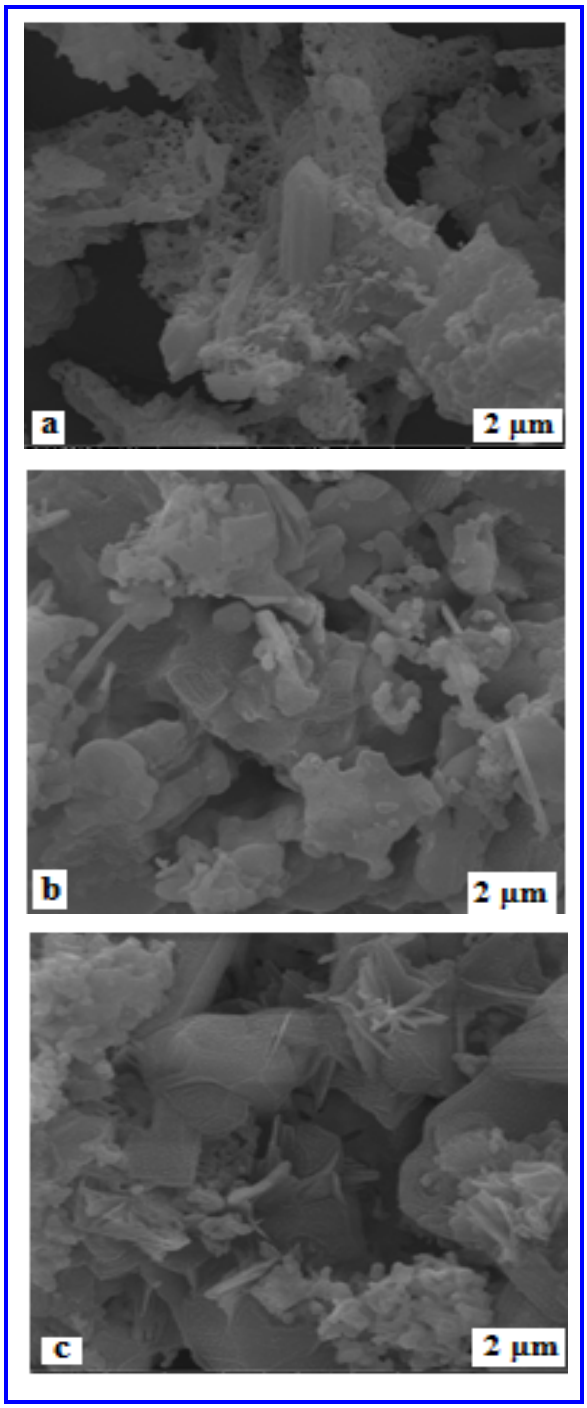

Fig 4. 2 SEM photograph of $Sm_{1-x}Sr_xAlO_3$

4.3. Thermal Analysis (TGA/DTA)

$Sm_{1-x}Sr_xAlO_3$nano crystalline powder has been studied before calcination with thermo gravimetric analysis (TGA) in air is shown in Fig. 4.3. The fig 4.3. Showed that thermal decomposition as completed at 700–750 °C. The first decomposition stage up to 250°C can be assigned to the loss of adsorbed water1 (Da Corte and Da Conceicao, 2013), the second stage at about 350–450 °C can be associated with the decomposition of combustion residues that are not burnt during the fast combustion reaction and the third stage at about 500°C can be observed the dissociation of carbonates during the combustion and starting of the formation of $Sm_{0.5}Sr_{0.5}AlO_3$ phase. Fig.4.3 shows the corresponding DTA curve for the synthesized powders. For the samples prepared by this method with aspartic acid, endothermic peaks are observed with more intense at 550 °C, which indicated the decomposition of organic residues (Ghosh et al. 2005).

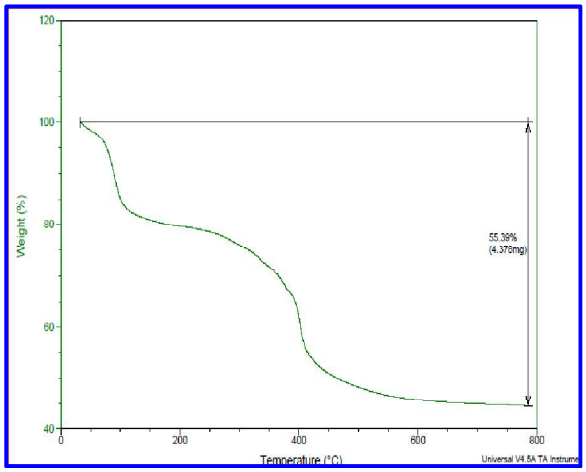

Fig. 4.3 TGA &DTA of $Sm_{0.5}Sr_{0.5}AlO_3$

4.4 FTIR Analysis

FTIR spectroscopy was used to confirm the functional groups present in the crystal and is investigated their vibrational behavior in solid state of $Sm_{1-x}Sr_xAlO_3$ powder, it was recorded in the range of 4000 cm^{-1} to 400cm^{-1}. The infrared spectrums of synthesized samples of $Sm_{0.5}Sr_{0.5}AlO_3$ powder are shown in fig.4.4. The broad band at 1472.0 cm^{-1} can be assigned to vibration mode of chemically bonded hydroxyl groups. The powder exhibited a strong bond at 500-800 cm^{-1} due to the stretching mode of Al bond in the structure. The peak appeared at 819.1 cm^{-1} corresponds to the H-O-H bond mode confirming the presence of moisture in the sample. The peak appeared

at 1410.9 cm $^{-1}$ is due to the presence of CO_2 in the sample. The sample $Sm_{0.5}Sr_{0.5}AlO_3$exhibited a low intensity peak at 754.5 cm $^{-1}$ and the sample exhibited three peaks obtained between the wavelength regions 800-1000 cm^{-1} and observed at 891.1, 1091.1 cm $^{-1}$. The peak appeared at 1541.8 cm^{-1} is related to the O-H stretching vibration of H_2O in the sample. The broad band at 1472.8 cm^{-1} can be assigned to vibration mode of chemically bonded hydroxyl groups.

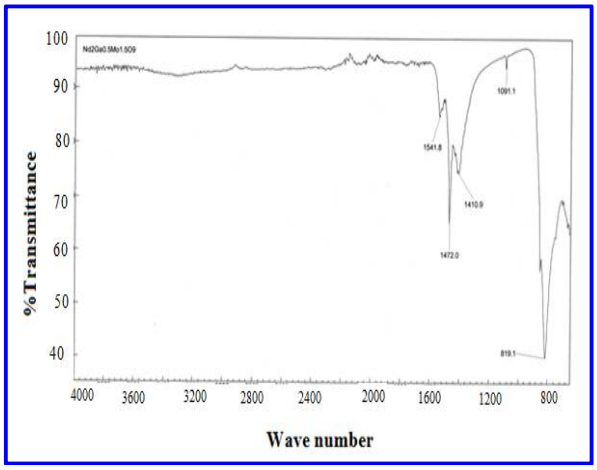

Fig. 4.4: FT-IR spectrum of $Sm_{0.5}Sr_{0.5}AlO_3$

4.6 Conductivity studies

Arrhenius plot of conductivity of the $Sm_{1-x}Sr_xAlO_3$samples are shown in Fig 4.5.

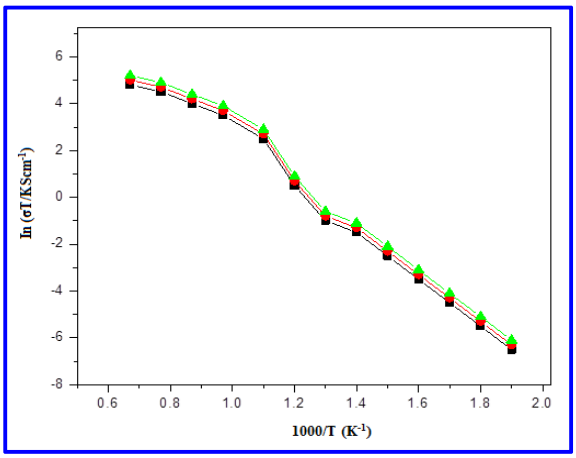

Fig. 4.5: Arrhenius plot for overall conductivity for $Sm_{1-x}Sr_xAlO_3$ sample

For pure $SmAlO_3$, a dramatic change of conductivity occurs at around 566˚C and is due to a phase transition. The Sr-doped $SmAlO_3$ samples exhibit slightly improved conductivity at lower and higher temperatures. Generally, the higher unit - cell free volume in the oxide ion conductor is easier for the oxygen-ion diffusion. On Sr – doping, the cell parameter is decreased. Thus, the substitution of Sr greatly increases the free volume and therefore the ionic conductivity of Sr-doped samples also increases remarkably. It can also be seen that a sharp conduction increases up to x=0.5 in $Sm_{1-x}Sr_xAlO_3$. The $Sm_{1-x}Sr_xAlO_3$sample exhibits on conductivity of 0.166 S cm^{-1} at 800°C, it compared with 0.12 S cm^{-1} for the undoped$SmAlO_3$. This result conformed that Al-doping can improve the oxide ion conductivity of $SmAlO_3$ at low and high temperatures. Moreover, the high purity and phase homogeneity of the present sample could help to improve the conductivity of Al-doped $SmAlO_3$ samples.

5. CONCLUSION

The present investigation was carried out to improve the performance of $Sm_{1-x}Sr_xAlO_3$by the synthesis method. The electrochemical behavior of $Sm_{1-x}Sr_xAlO_3$ based materials depend on the method of synthesis and sintering temperature. The present work was mainly focused on synthesis, and ionic conductivity $Sm_{1-x}Sr_xAlO_3$.

REFERENCES

Bansal, N. P. and Zhong, Z., Combustion synthesis of Sm0.5Sr0.5CoO3−x and La0.6Sr0.4CoO3−x nanopowders for solid oxide fuel cell cathodes, J. Power Sources, 158, 148–153(2006).

Berger, D., Matei, C., Papa, F., Macovei, D., Fruth, V. and Deloume, J. P., Pure and doped lanthanum manganites obtained by combustion method, J. Eur. Ceram. Soc. 27, 4395–4398(2007).

Da Corte, R. V., Da Conceicao, L. and Souza, M. M. V. M., Structural and electrical properties of La0.7Sr0.3Co0.5Fe0.5O3 powers synthesized by solid state reaction, Ceram. Int. 39, 7975–7982(2013).

Fang, Q, F., Wang, X. P., Li., Z. S., Zhang, G. G. and Yi, Z. G., Relaxation peaks associated with the oxygen-ion diffusion in $La_{2-x}Bi_xMo_2O_9$ oxide ion conductors, Material science and Engineering A, 370, 365-369(2004).

Ghosh, A., Sahu, A. K., Gulnar, A. K. and Suri, A. K., Synthesis and characterization of lanthanum strontium manganite, Scr. Mater., 52, 1305–1309(2005).

John B. Goodenongh, Yun-Hui Huang, Alternative anode materials for solid oxide fuel cells, Journal of power source, 173, 1-10(2007).

Minh, N. Q. and Takahashi, T., Science and technology of Ceramic Fuel Cells; Elsevier, Amsterdam, 1995.

Shoucheng He, Han Chen, Ruifeng Li, Lin Ge, LucunGuo, Effect of $Ce_{0.8}Sm_{0.2}O_{1.9}$ inter layer on the electrochemical performance of $La_{0.75}Sr_{0.25}Cr_{0.5}Mn_{0.5}O_{3-\delta}$-$Ce_{0.8}Sm_{0.2}O_{1.9}$ composite anodes for intermediate-temperature solid oxide fuel cells, Journal of power source, 253, 187-192(2014).

Singh, P., Pederson, L. R., Simner, S. P., Stevenson, J. W. and Viswanathan, V. V., Proceedings of the 36th Intersociety Energy Conversion Engineering Conference, Savannah, GA, July 29-Aug 2, 2001; American Society of Mechanical Engineers; New York, 2, 953-958(2001).

Singhal, S. C. H. and Yokokawa, H, Solid oxide fuel cells VII: proceeding of the seventh international Symposium; Tsukumba, Japan, June 2001; The electrochemical society: pennington,NJ, 2001.

Singhal, S. C., Advances in solid oxide fuel cell technology, Solid State Ionics, 135, 305-313(2000).

Steele, B.C.H. and Heinzel, A., Nature, 414, 345-353(2001).

Stuart A Hayward and Simon A T Redfern, Thermodynamic nature of and spontaneous strain below the cubic–monoclinic phase transition in $La_2Mo_2O_9$, J. Phys., Condens. Matte, 16, 3571–3583(2004).

Young-Hag Koh, Jong-Jae Sun, Won-Young Choi, Hyoun-Ee Kim, Design and fabrication of three-dimensional solid oxide fuel cells, Journal of power sources, 161, 1023-1029(2006).